

1                   **Comparison of nickel adsorption on biochars produced from mixed**  
2  
3                   **softwood and *miscanthus* straw**

4  
5  
6  
7                   Zhengtao Shen <sup>a, b, 1, \*</sup>, Yunhui Zhang <sup>a, 1</sup>, Fei Jin <sup>c</sup>, Daniel S. Alessi <sup>b</sup>, Yiyun  
8  
9                   Zhang <sup>a</sup>, Fei Wang <sup>a, d, \*</sup>, Oliver McMillan <sup>a</sup>, Abir Al-Tabbaa <sup>a</sup>

10  
11  
12  
13                   <sup>a</sup> Geotechnical and Environmental Research Group, Department of  
14                   Engineering, University of Cambridge, Cambridge CB2 1PZ, United Kingdom

15  
16  
17  
18                   <sup>b</sup> Department of Earth and Atmospheric Sciences, University of Alberta,  
19                   Edmonton T6G 2E3, Canada

20  
21  
22                   <sup>c</sup> School of Engineering, University of Glasgow, Glasgow G12 8QQ, UK

23  
24  
25  
26                   <sup>d</sup> Institute of Geotechnical Engineering, School of Transportation, Southeast  
27                   University, Nanjing 210096, China

28  
29  
30                   \* Corresponding author:

31  
32  
33                   Zhengtao Shen, Email: [ztshennju@gmail.com](mailto:ztshennju@gmail.com); [zshen4@ualberta.ca](mailto:zshen4@ualberta.ca)

34  
35                   & Fei Wang, Email: [101012020@seu.edu.cn](mailto:101012020@seu.edu.cn)

36  
37  
38                   <sup>1</sup> These authors contributed equally to this work

1 Abstract: In order to understand the influence of feedstock type on biochar  
2  
3 adsorption of heavy metals, the adsorption characteristics of nickel ( $\text{Ni}^{2+}$ ),  
4  
5 copper ( $\text{Cu}^{2+}$ ) and lead ( $\text{Pb}^{2+}$ ) onto biochars derived from mixed softwood and  
6  
7 *miscanthus* straw were compared. The biochars were produced from mixed  
8  
9 softwood pellets (SWP) and *miscanthus* straw pellets (MSP), at both 550 °C  
10  
11 and 700 °C for each material, using a standardised production procedure  
12  
13 recommended by the UK Biochar Research Centre. Kinetics analyses show  
14  
15 that the adsorption of  $\text{Ni}^{2+}$  to all four biochars reached equilibrium within 5  
16  
17 minutes. The degree of  $\text{Ni}^{2+}$  removal for all four biochars remained nearly  
18  
19 constant within initial pH values of 3-8, because the equilibrium pH values  
20  
21 within this range were similar due to the buffering effect of the biochars. A  
22  
23 sharp increase of  $\text{Ni}^{2+}$  removal percentage for all biochars at initial solution pH  
24  
25 8-10 was observed as the equilibrium pH also increased. MSP derived  
26  
27 biochars generally had higher maximum adsorption capacities ( $Q_{\text{max}}$ ) for the  
28  
29 three tested metals as compared with those from SWP, which was likely due to  
30  
31 their higher degree of carbonisation during production. This study shows that  
32  
33 feedstock type is a primary factor affecting the adsorption capacities of the  
34  
35 tested biochars for heavy metals.  
36  
37  
38  
39  
40  
41  
42  
43  
44  
45  
46  
47  
48  
49  
50

51  
52  
53 Keywords: biochar, remediation, adsorption, heavy metal, softwood,  
54  
55 *miscanthus* straw  
56  
57  
58

## 1 Introduction

Environmental pollution in air, land, and water has been a huge challenge to the modern society (Hou and Li 2017; Qi et al. 2017; P. Zhang et al. 2017). The sustainable remediation of contaminated environmental media has drawn great attention during recent years (Hou and Al-Tabbaa 2014; Hou et al. 2017a; Hou et al. 2017b; Song et al. 2018). Biochar is regarded as an emerging and sustainable sorbent for heavy metal remediation of water and soil, due to its multiple additional environmental benefits including waste management, energy production, carbon storage and soil improvement (Ronsse et al. 2013; Lehmann 2007; Cao et al. 2011; Beesley et al. 2011; Shen et al. 2016; Shen et al. 2017a). Key to applying biochar for these purposes is an understanding of the adsorption characteristics of heavy metals, in order to aid in its practical application in water and soil remediation.

Biochar properties are highly dependent on the type of feedstock used (Zhang et al. 2017a). Plant, sewage sludge, manure and bones are raw materials often used for biochar production (Li et al. 2017), and plants obtained from agriculture wastes are among the most typical types of biomass used as biochar feedstock. Plants mainly consist of lignin, cellulose, hemicellulose and inorganic minerals, and the content of each component varies as a function of the plant type. Taking wood and wheat straw, two of the most frequently used

1 feedstocks for biochar, as examples, wood contains more lignin (25-30% for  
2  
3 wood versus 15-20% for wheat straw) and less inorganic minerals than does  
4  
5 straw (Jahirul et al. 2012). The differing thermal decomposition patterns of  
6  
7 each component during heating (Jahirul et al. 2012) results in biochars with  
8  
9 significantly different properties and consequently differing metal adsorption  
10  
11 behaviours. Heavy metal is an important class of environmental pollutants that  
12  
13 may originate from various anthropogenic sources and are widely distributed  
14  
15 (Hou et al. 2016, 2017c; Ma et al. 2015, 2014). A range of laboratory studies  
16  
17 have revealed the adsorption characteristics of heavy metals on biochars  
18  
19 produced from a particular plant biomass (e.g., Park et al. 2015; Shen et al.  
20  
21 2015; Chi et al. 2017). However, the biochar production parameters, including  
22  
23 highest heating temperature, heating rate, residence time, protection gas and  
24  
25 quality control, vary widely among these studies. It is therefore difficult to  
26  
27 isolate the influence of feedstock type on the adsorption of heavy metals by  
28  
29 biochar. Although comparison of the adsorption of heavy metals among  
30  
31 biochars, produced from different plant biomass under same conditions, has  
32  
33 been conducted in several previous studies (Wang et al. 2016; Mohan et al.  
34  
35 2007), it has not been extensively investigated, especially for biochars  
36  
37 produced under highly controlled pyrolysis conditions and having high  
38  
39 reproducibility.  
40  
41  
42  
43  
44  
45  
46  
47  
48  
49  
50  
51  
52  
53  
54  
55  
56  
57  
58  
59  
60  
61  
62  
63  
64  
65

1 In order to aid the selection of the most suitable biochars for treatment of  
2  
3 heavy metals in soil and water, it is critical to understand the influence of  
4  
5 feedstock type on biochar adsorption of heavy metals after eliminating other  
6  
7 influencing factors. To that end, in this study, mixed softwood and *miscanthus*  
8  
9 straw biochars were obtained from the UK Biochar Research Centre (UKBRC),  
10  
11 which aims to produce standardised biochars. A high degree of reproducibility  
12  
13 of these standard biochars can be achieved because the production process  
14  
15 and pyrolysis conditions are carefully monitored. This enables to isolate in the  
16  
17 current study the influence of feedstock type on biochar adsorption of three  
18  
19 tested metals: nickel (Ni<sup>2+</sup>), copper (Cu<sup>2+</sup>) and lead (Pb<sup>2+</sup>), using laboratory  
20  
21 batch adsorption experiments.  
22  
23  
24  
25  
26  
27  
28  
29  
30

## 31 32 33 2 Materials and methods 34 35

### 36 37 2.1 Biochar 38 39

40 Two types of feedstock biomass were used to produce the biochar used in this  
41  
42 study: (1) mixed softwood pellets (SWP) and, (2) *miscanthus* straw pellets  
43  
44 (MSP). Biochars were produced by the United Kingdom Biochar Research  
45  
46 Centre (UKBRC) from both SWP and MSP at both 550 °C and 700 °C,  
47  
48 resulting in four biochars hereafter referred to as SWP550, SWP700, MSP550  
49  
50 and MSP700. The standardised production procedure can be found on the  
51  
52 website of UKBRC (UKBRC 2016). Upon receipt, the biochars were dried in an  
53  
54  
55  
56  
57  
58  
59

1 oven at 60 °C for 48 h and sieved to < 0.15 mm particle sizes before  
2  
3  
4 experimentation. The cation exchange capacity (CEC) of each biochar was  
5  
6 tested using a compulsive exchange method based on Gillman and Sumpter  
7  
8 (1986). Other physicochemical properties were obtained from the UKBRC  
9  
10 (2016). The surface morphology of the biochar was examined by a scanning  
11  
12 electron microscopy (SEM) at 15 kV after coating the samples with gold. The  
13  
14 infrared spectrum of each biochar before and after Ni<sup>2+</sup> adsorption was  
15  
16 obtained using a TENSOR II Fourier transform infrared spectroscopy (FT-IR)  
17  
18 spectrometer (Bruker), by taking 16 scans from 2000 to 700 cm<sup>-1</sup> with a  
19  
20 resolution of 1 cm<sup>-1</sup>.  
21  
22  
23  
24  
25  
26  
27  
28

29  
30 According to tests conducted by the UKBRC, the biochars predominantly  
31  
32 consist of carbon (75.41-90.21%) (Table 1). SWP derived biochars have  
33  
34 considerably lower pH than do those produced from MSP (7.91-8.44 versus  
35  
36 9.72-9.77). All four biochars are alkaline, with pH<sub>pzc</sub> (point of zero charge)  
37  
38 values between 7.8-7.9 (pH<sub>pzc</sub> values can be obtained from adsorption study  
39  
40 results of Mohan et al. (2014)). SWP derived biochars contain very low ash  
41  
42 content (1.25-1.89%), while the content in MSP biochars is much higher  
43  
44 (11.55-12.15%). Likewise, SWP derived biochars have lower P contents than  
45  
46 MSP (0.06-0.07% versus 0.19-0.76%). The CECs and surface areas of the  
47  
48 biochars are relatively low as compared with existing literature (Cui et al. 2015;  
49  
50  
51  
52  
53  
54  
55  
56  
57  
58  
59  
60  
61  
62  
63  
64  
65

1 Chotpantararat et al. 2011), except for SWP700 which has a relatively high  
 2  
 3 surface area (162.30 m<sup>2</sup> g<sup>-1</sup>) suggesting a porous structure.  
 4  
 5  
 6

7 Table 1 Physicochemical properties of the biochars  
 8  
 9

	SWP550	SWP700	MSP550	MSP700
C (%)	85.52	90.21	75.41	79.18
H (%)	2.77	1.83	2.42	1.26
O (by difference) (%)	10.36	6.02	9.24	6.99
N (%)	<0.10	<0.10	0.78	1.03
P (%)	0.06	0.07	0.19	0.76
VM (%)	14.20	6.66	11.62	7.71
H:C	0.39	0.24	0.38	0.19
O:C	0.09	0.05	0.09	0.07
Total ash (%)	1.25	1.89	12.15	11.55
pH	7.91	8.44	9.77	9.72
pH <sub>pzc</sub> *	7.8	7.9	7.8	7.8
BET surface area (m <sup>2</sup> /g)	26.40	162.30	33.60	37.20
CEC (cmol/kg) *	2.53	2.56	5.95	10.80
Ni (mg/kg)	3.30	74.07	30.40	4.95
Cu (mg/kg)	19.41	9.66	26.64	5.88
Pb (mg/kg)	bdl	bdl	bdl	bdl

1 (VM = volatile matter,  $\text{pH}_{\text{PZC}}$  = point of zero charge, BET = Brunauer–Emmett–Teller, CEC  
2  
3  
4 = cation exchange capacity, bdl = below detection limit, the standard deviations (SD) for  
5  
6 CEC were within 0.10-0.23, the SD for other properties can be found on UKBRC (2016),  
7  
8  
9 note that all the values are obtained from the UKBRC datasheet, except for those denoted  
10  
11  
12 with \*)  
13

## 14 2.2 Adsorption studies

15  
16  
17  
18  
19  $\text{Ni}^{2+}$ ,  $\text{Cu}^{2+}$  and  $\text{Pb}^{2+}$  were used as model divalent cations, to investigate the  
20  
21  
22 sorption of heavy metals to these biochars. The kinetics and both the influence  
23  
24  
25 of **adsorbent dosage** and solution pH on  $\text{Ni}^{2+}$  uptake from solution for all four  
26  
27  
28 biochars were investigated. The equilibrium adsorption of  $\text{Ni}^{2+}$ ,  $\text{Cu}^{2+}$  and  $\text{Pb}^{2+}$   
29  
30  
31 onto each of the biochars was also investigated.  
32

33  
34  
35 Batch adsorption experiments were carried out in 50 mL polyethylene tubes in  
36  
37  
38 a temperature-controlled laboratory ( $20 \pm 1$  °C). The detailed experimental  
39  
40  
41 procedure of the adsorption studies can be found in Shen et al. (2017b). Briefly,  
42  
43  
44 for kinetics studies, 0.1 g biochar was added to 20 mL solutions of 5 mM  
45  
46  $\text{Ni}(\text{NO}_3)_2$  (pH 5) (containing 0.01 M  $\text{NaNO}_3$ ) and shaken at 200 rpm for 5 min,  
47  
48  
49 10 min, 20 min, 30 min, 1 h, 2 h, 3 h, 6 h, 12 h or 24 h. The effect of **adsorbent**  
50  
51  
52 **dosage** on the equilibrium adsorption of  $\text{Ni}^{2+}$  was investigated by adding a  
53  
54  
55 measured amount of biochar (0.1, 0.2, 0.3, 0.4, 0.5, 0.6, 0.7, 0.8, 0.9 or 1 g) to  
56  
57  
58 20 mL of 5 mM  $\text{Ni}(\text{NO}_3)_2$  (containing 0.01 M  $\text{NaNO}_3$ ) set to pH 5, and shaking  
59



1 those mixtures at 200 rpm for 24 h. The effect of solution pH on Ni<sup>2+</sup> adsorption  
2  
3 was investigated by adding 0.1 g of biochar to solutions containing 20 mL of 5  
4  
5 mM Ni(NO<sub>3</sub>)<sub>2</sub> (containing 0.01 M NaNO<sub>3</sub>), and subsequently shaking at 200  
6  
7 rpm for 24 h. The initial pH of each solution (before biochar addition) was  
8  
9 adjusted to 2, 3, 4, 5, 6, 7, 8, 9 or 10. Solutions of 0.01M, 0.1 M and 1 M HNO<sub>3</sub>  
10  
11 and 0.01M, 0.1 M and 1M NaOH were used to adjust the initial pH of the  
12  
13 solutions where required. The equilibrium pH and the removal of Ni<sup>2+</sup> were  
14  
15 recorded. In order to distinguish between precipitated Ni(OH)<sub>2</sub> and adsorbed  
16  
17 Ni<sup>2+</sup> as a function of equilibrium pH, the fractions of Ni<sup>2+</sup> removed via  
18  
19 precipitation were calculated using Visual MINTEQ 3.1.  
20  
21  
22  
23  
24  
25  
26  
27  
28  
29

30 In order to construct metal adsorption isotherms for each biochar, 0.1 g biochar  
31  
32 was added to 20 mL solutions (pH = 5) containing either Ni<sup>2+</sup>, Cu<sup>2+</sup> or Pb<sup>2+</sup>, at  
33  
34 concentrations of 0.1, 0.2, 0.3, 0.5, 1, 2, 3 or 5 mM (containing 0.01 M NaNO<sub>3</sub>).  
35  
36 The resulting mixtures were shaken at 200 rpm for 24 h to reach equilibrium.  
37  
38 The equilibrium data were fit using linearized Langmuir and Freundlich models  
39  
40 to reveal the maximum adsorption capacities and adsorption mechanisms of  
41  
42 the metals on the biochars, as suggested by (Foo and Hameed 2010). The  
43  
44 details of the models and calculations are given in Table S1.  
45  
46  
47  
48  
49  
50  
51  
52  
53

### 54 2.3 Statistical analysis

55  
56

57 All experiments were conducted in duplicates, and the means and standard  
58  
59

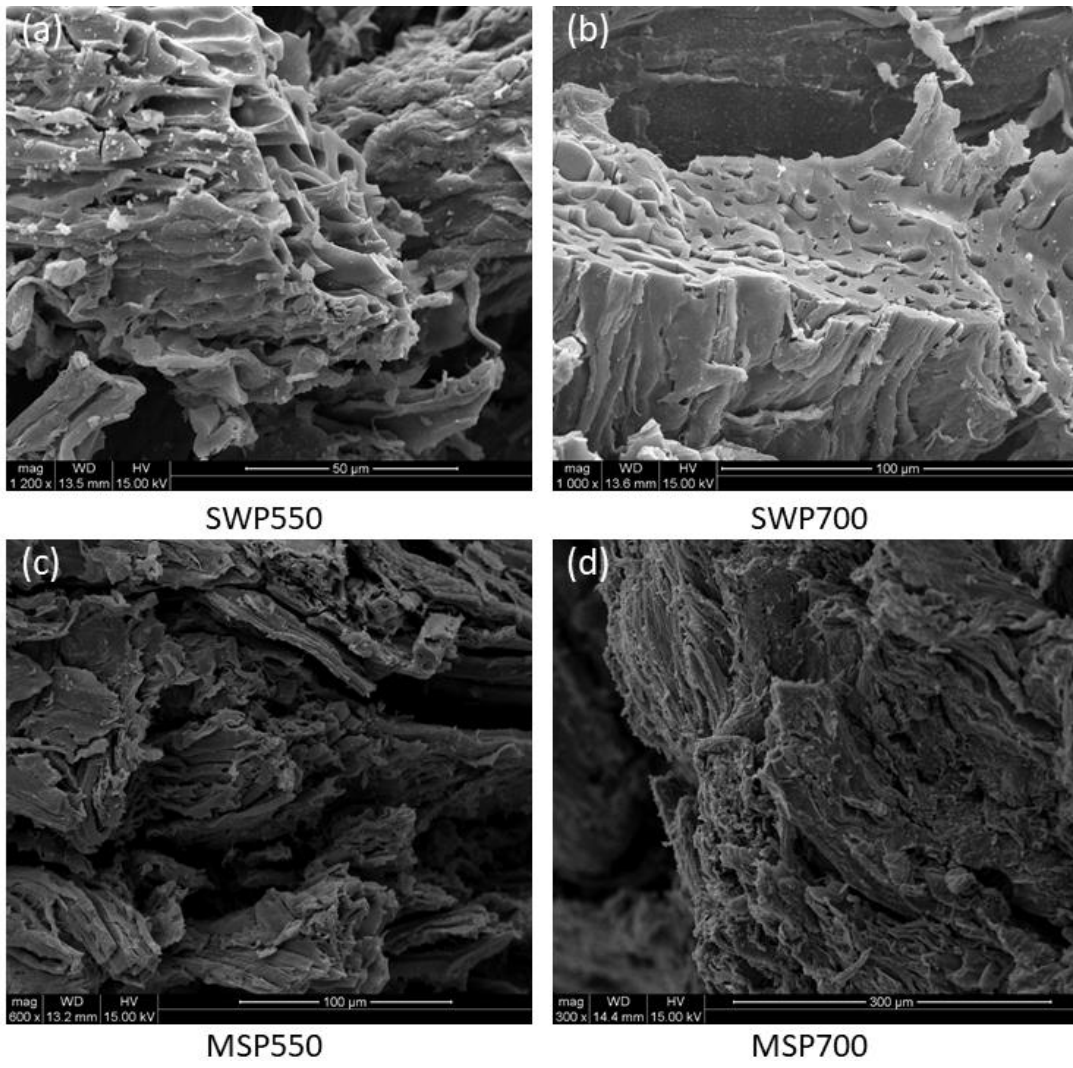
1 deviations were calculated from these data. Linear regression was used to  
2  
3 evaluate the fitness of the prediction models to the experimental data in this  
4  
5 study using Origin 8.5. The suitability of the model fitting was assessed using  
6  
7  
8  
9  $R^2$  values.  
10

### 11 12 13 3 Results and discussion

#### 14 15 16 3.1 FT-IR spectra and SEM images of biochars

17  
18  
19  
20 The FT-IR spectra of the biochars are shown in Fig. 5. The peaks at  $1575\text{ cm}^{-1}$   
21  
22 for SWP550 and MSP550 are attributed to aromatic C=C stretching (Keiluweit  
23  
24 et al. 2010), and the peaks at  $875$ ,  $800$  and  $750\text{ cm}^{-1}$  for SWP550 and MSP550  
25  
26 are attributed to aromatic C-H bending (Keiluweit et al. 2010), indicating an  
27  
28 aromatic structure of the two biochars. Less peaks associated with aromatic C  
29  
30 were observed on SWP700 and MSP700, suggesting that more condensed  
31  
32 aromatic structure with less functional groups was formed, as increased peak  
33  
34 temperature. The big peak between  $1030$ - $1080\text{ cm}^{-1}$  for MSP550 is attributed  
35  
36 to C-O-C stretching vibrations resulted from cellulose and hemicellulose  
37  
38 (Keiluweit et al. 2010). With increased peak temperature, cellulose and  
39  
40 hemicellulose in the *miscanthus* straw further decomposed, resulting in less  
41  
42 C-O-C groups. Therefore, this big peak diminished on FT-IR spectra of  
43  
44 MSP700. Wood typically contain less cellulose and hemicellulose and more  
45  
46 lignin than straw (Jahirul et al. 2012), therefore, the C-O-C peak was not  
47  
48  
49  
50  
51  
52  
53  
54  
55  
56  
57  
58  
59  
60  
61  
62  
63  
64  
65

1 obvious for SWP derived biochars, or the cellulose and hemicellulose already  
2  
3 decomposed due to less amount. The SEM images (Fig. 1) show the porous  
4  
5 structures of the four biochars, which is typical for plant-derived biochars  
6  
7  
8  
9 (Usman et al. 2016). The pore diameters are generally less than 5  $\mu\text{m}$  for all  
10  
11  
12 biochars. MSP derived biochars generally reveal smaller pores than WSP. The  
13  
14 differences in the morphology due to production temperature were not  
15  
16  
17  
18 obvious.  
19  
20  
21  
22



1 Fig. 1. SEM images of the biochars, including: (a) SWP550, (b) SWP700, (c)  
2  
3  
4 MSP550, and (d) MSP700.  
5  
6

### 7 3.2 Kinetics 8 9

10 The adsorption of Ni<sup>2+</sup> to the four biochars reached equilibrium within 5  
11 minutes (Fig. 2). Both the relatively high initial solution Ni<sup>2+</sup> concentration (5  
12 mM) and the fine biochar particle size (< 0.15 mm) likely contributed to this  
13 rapid adsorption. Higher adsorbate concentration in solution results in a larger  
14 chance for contact between the adsorbate and adsorbent surface, and  
15 therefore accelerated movement of adsorbate across the external liquid film  
16 boundary layer to external surface sites of the adsorbent (film diffusion) (Choy  
17 et al. 2004). Smaller particles have larger **specific** surface area, which may  
18 also aids the speed of film diffusion due to a larger solid – aqueous interface  
19 (Choy et al. 2004). In addition, the mass transport of adsorbate inside the  
20 adsorbent (intraparticle diffusion) becomes shorter as the radius of the  
21 adsorbent particle decreases, which also makes the adsorption faster (Choy et  
22 al. 2004; Rees et al. 2014). The rapid adsorption rate also suggests  
23 chemisorption (e.g. surface precipitation) may be a predominant mechanism  
24 for Ni<sup>2+</sup> adsorption onto the four biochars, as chemisorption typically takes a  
25 shorter time, often within minutes (Inyang et al. 2015; Saleh et al. 2016; Tran et  
26 al. 2016).  
27  
28  
29  
30  
31  
32  
33  
34  
35  
36  
37  
38  
39  
40  
41  
42  
43  
44  
45  
46  
47  
48  
49  
50  
51  
52  
53  
54  
55  
56  
57  
58  
59  
60  
61  
62  
63  
64  
65

1 The adsorption capacities ( $q_e$ ) of  $\text{Ni}^{2+}$  on WSP550 and WSP700 were not  
2 significantly different, with both values between 0.03 and 0.05 mmol/g. In  
3  
4  
5  
6  
7  
8  
9  
10  
11  
12  
13  
14  
15  
16  
17  
18  
19  
20  
21  
22  
23  
24  
25  
26  
27  
28  
29  
30  
31  
32  
33  
34  
35  
36  
37  
38  
39  
40  
41  
42  
43  
44  
45  
46  
47  
48  
49  
50  
51  
52  
53  
54  
55  
56  
57  
58  
59  
60  
61  
62  
63  
64  
65

The adsorption capacities ( $q_e$ ) of  $\text{Ni}^{2+}$  on WSP550 and WSP700 were not significantly different, with both values between 0.03 and 0.05 mmol/g. In contrast, the  $q_e$  values for MSP derived biochars were significantly higher. The  $q_e$  for MSP700, around 0.35 mmol/g, was nearly double that of MSP550, suggesting that a higher production temperature aids in the adsorption capacity of MSP derived biochars.

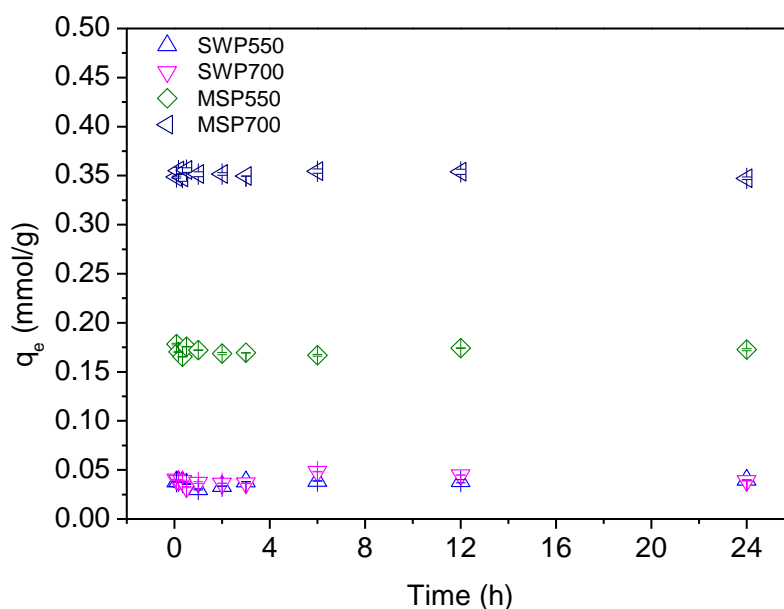


Fig. 2. Kinetics of  $\text{Ni}^{2+}$  adsorption on biochars (0.1 g biochar in 20 mL solution (0.01 M  $\text{NaNO}_3$ ), initial  $\text{Ni}^{2+}$  concentration 5 mM; reaction temperature 20 °C; initial solution pH 5) ( $q_e$  - adsorption capacities).

### 3.3 Influence of adsorbent dosage

The influences of adsorbent dosage on Ni<sup>2+</sup> removal and the adsorbed amount of Ni<sup>2+</sup> per weight unit of biochar are shown in Fig. 3. The Ni<sup>2+</sup> removal percentage for SWP550 increased from 3.97% to 16.63% across the adsorbent dosage range of 5-50 g/L. Likewise, the Ni<sup>2+</sup> removal percentage for SWP700 increased from 3.89% to 20.54% at this range. Both biochars did not reach complete Ni<sup>2+</sup> removal at the range of 5-50 g/L and exhibited low removal percentages compared with MSP derived biochars, suggesting a relatively low adsorption capacity of Ni<sup>2+</sup> on SWP derived biochars. The adsorbed amount of Ni<sup>2+</sup> per weight unit of biochar decreased in the range of 5-50 g/L for both of the SWP derived biochars.

In comparison to SWP derived biochars, the Ni<sup>2+</sup> removal percentage for MSP550 increased from 17.28% to 98.03% as the adsorbent dosage increased from 5 to 40 g/L and remained at approximately 100% removal in the range of 40-50 g/L. The Ni<sup>2+</sup> removal percentage for MSP700 increased from 18.29% to 99.67% at the adsorbent dosage range of 5-35 g/L and remained close to 100% removal up to 50 g/L. The adsorbed amount of Ni<sup>2+</sup> per unit weight of biochar decreased as the adsorbent dosage increased from 5 to 50 g/L for both biochars. MSP-derived biochars generally show higher Ni<sup>2+</sup> removal ability compared with SWP-derived biochars, which is in line with the

kinetics findings.

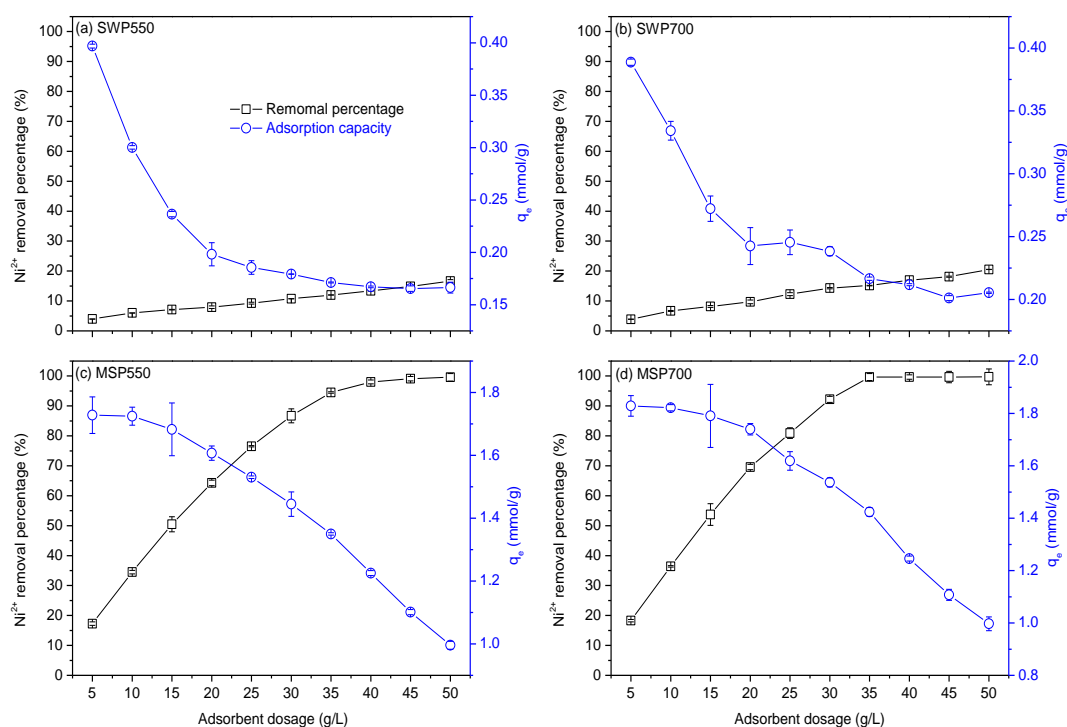


Fig. 3. The influence of adsorbent dosage on Ni<sup>2+</sup> removal percentage and the adsorbed amount of Ni<sup>2+</sup> per weight unit of biochar (mmol/g) (initial Ni<sup>2+</sup> concentration 5mM in 20 mL solution (containing 0.01 M NaNO<sub>3</sub>), reaction temperature 20 °C, initial solution pH 5, contact time 24 h).

### 3.4 Influence of solution pH

The influences of the initial solution pH on Ni<sup>2+</sup> removal percentage and equilibrium solution pH values are shown in Fig. 4. The fraction of Ni<sup>2+</sup> removed due to precipitation is also shown, which was calculated from the Ni(OH)<sub>2</sub> solubility data from the MINTEQ database. The high p<sub>H<sub>pzc</sub></sub> (7.8-7.9)

1 suggests that the strong alkalinity of the biochars will aid in their adsorption for  
2  
3 heavy metals through surface precipitation. It is of note that the pH near the  
4  
5 biochar surface may be higher than the solution pH itself, and so even at lower  
6  
7 solution pH, surface precipitation of metals may already have occurred.  
8  
9 Therefore, there may be a discrepancy between the measured equilibrium  
10  
11 solution pH and the conditions of precipitation calculated using MINTEQ.  
12  
13  
14  
15  
16  
17

18 The Ni<sup>2+</sup> removal percentage for SWP derived biochars was low (3-5%) in the  
19  
20 initial solution pH range of 2-7. It increased slightly to 9.82% at initial pH 8  
21  
22 before sharply increasing to 85.14% at initial pH 9 and subsequently increased  
23  
24 to 99.50% at initial solution pH 10 for SWP550. For SWP700, it stayed within  
25  
26 3-5% at pH 8 and sharply increased to 85.82% at pH 9. It further increased to  
27  
28 99.79% at initial pH 10. The Ni<sup>2+</sup> removal percentage for MSP550 increased  
29  
30 from 3.41% to 15.44% as the initial solution pH increased from 2 to 4. It stayed  
31  
32 nearly constant at the initial pH range of 4-8 before significantly increasing to  
33  
34 98.45% at initial pH 9, and remained at nearly complete removal at initial pH  
35  
36 10. The Ni<sup>2+</sup> removal percentage for MSP700 increased from 1.56% to 18.14%  
37  
38 with the increase of initial solution pH from 2 to 4. It was nearly constant within  
39  
40 the initial pH range of 4-7 and slightly increased to 33.33% at pH 8. A sharp  
41  
42 increase occurred between initial solution pH 8-9, nearing complete removal at  
43  
44 initial pH 9-10. The changes in the precipitation of Ni(OH)<sub>2</sub> did not have a  
45  
46  
47  
48  
49  
50  
51  
52  
53  
54  
55  
56  
57  
58  
59  
60  
61  
62  
63  
64  
65



1 significant effect on Ni<sup>2+</sup> removal between pH 2 and 9.

2  
3  
4 The Ni<sup>2+</sup> removal percentages for SWP derived biochars were closely related  
5  
6  
7 to the equilibrium solution pH values. The Ni<sup>2+</sup> removal percentages remained  
8  
9  
10 nearly constant within initial pH values of 3-8, because the equilibrium pH  
11  
12  
13 values at this range were relatively stable resulting from the buffering effect of  
14  
15  
16 the biochars. The insignificant increase of Ni<sup>2+</sup> removal percentages at initial  
17  
18  
19 pH 2-4 for SWP derived biochars was likely due to proton competition with Ni<sup>2+</sup>  
20  
21  
22 for adsorption onto biochar surface functional groups (Uchimiya et al. 2012).  
23  
24  
25 The sharp increase of Ni<sup>2+</sup> removal percentage for all biochars at initial  
26  
27  
28 solution pH 8-10 likely occurred because the p*H*<sub>pzc</sub> values of the biochars were  
29  
30  
31 exceeded. Under these conditions, the biochar surfaces became negatively  
32  
33  
34 charged, which enhanced adsorption of Ni<sup>2+</sup> through electrostatic interactions.  
35  
36  
37 In addition, Ni(OH)<sub>2</sub> starts to precipitate on biochar surfaces at this range,  
38  
39  
40 which likely also contributed to the sharp increase of Ni<sup>2+</sup> removal from  
41  
42  
43  
44  
45  
46  
47  
48  
49  
50  
51  
52  
53  
54  
55  
56  
57  
58  
59  
60  
61  
62  
63  
64  
65

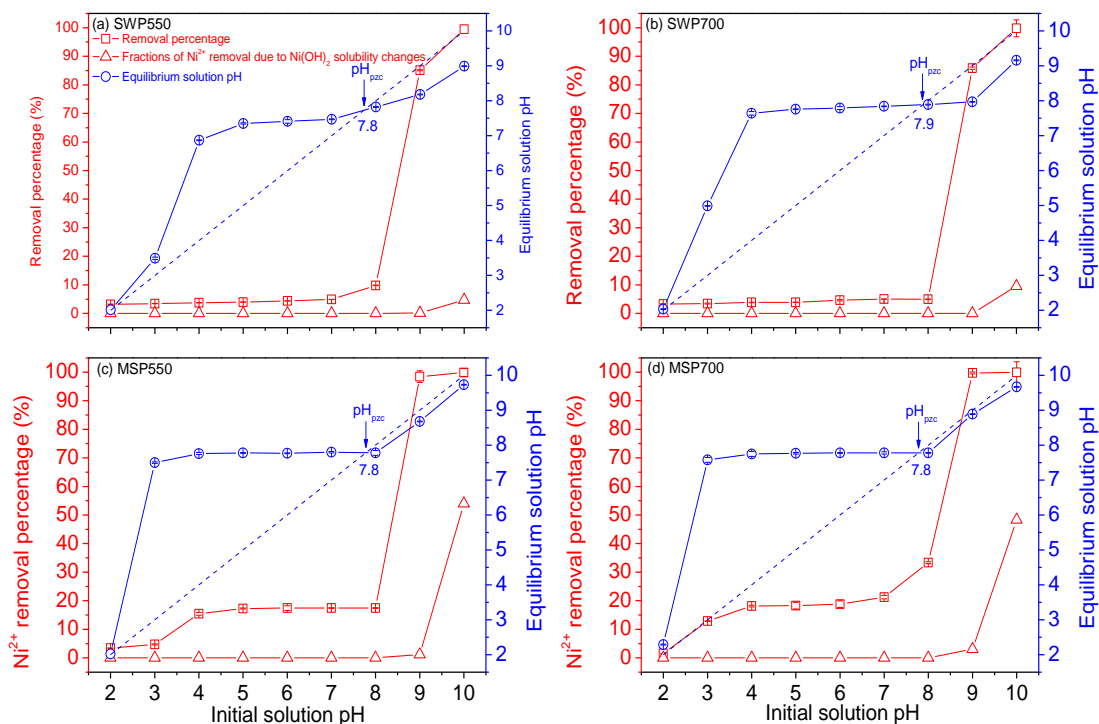


Fig. 4. The influence of initial solution pH on the Ni<sup>2+</sup> removal percentage (red squares with solid lines), the equilibrium solution pH (blue circles with solid lines) and the fractions of Ni<sup>2+</sup> removal due to the solubility change of Ni(OH)<sub>2</sub> (red triangles with solid lines); the dashed line is used to obtain the pH<sub>pzc</sub> (initial Ni<sup>2+</sup> concentration 5 mM, 0.1 g biochar in 20 mL solution (containing 0.01 M NaNO<sub>3</sub>), reaction temperature 20 °C, contact time 24 h).

### 3.5 Adsorption equilibrium

Data from the equilibrium metal adsorption experiments conducted at room temperature for Ni<sup>2+</sup> adsorption on biochars were modelled using isotherm approaches. Those for Cu<sup>2+</sup> and Pb<sup>2+</sup> were also obtained for comparison (Figs. S1, S2, S3 and Table 2). All isotherms are better fit by the Langmuir model

1 than by the Freundlich model, except for Ni<sup>2+</sup> adsorption on MSP550 and  
 2  
 3 MSP700, indicating a monolayer adsorption of heavy metals on the biochars.  
 4  
 5 Ni<sup>2+</sup> adsorption on MSP550 and MSP700 reveals slightly higher R<sup>2</sup> values for  
 6  
 7 the Freundlich model than for the Langmuir model, suggesting a certain degree  
 8  
 9 of heterogeneity of the adsorption sites on MSP550 and MSP700 surfaces.  
 10  
 11 The maximum adsorption capacity (Q<sub>max</sub>) of heavy metals on biochars can be  
 12  
 13 calculated using the Langmuir model, and MSP derived biochars reveal  
 14  
 15 significantly higher Q<sub>max</sub> values than do SWP for all three metals (Table 2).  
 16  
 17 Pb<sup>2+</sup> generally has higher Q<sub>max</sub> values than do Ni<sup>2+</sup> and Cu<sup>2+</sup> on the MSP  
 18  
 19 derived biochars, due to its lower hydration energy, which coincides with many  
 20  
 21 previous findings (Shen et al. 2015; Liu et al. 2013). For SWP derived biochars,  
 22  
 23 the Q<sub>max</sub> values for the three metals vary considerably, and so there is not a  
 24  
 25 specific metal that has the highest Q<sub>max</sub> values.  
 26  
 27  
 28  
 29  
 30  
 31  
 32  
 33  
 34  
 35  
 36  
 37  
 38  
 39  
 40  
 41  
 42  
 43  
 44  
 45  
 46

39 Table 2 Parameters and regression coefficient of the equilibrium data for Ni<sup>2+</sup>,  
 40  
 41 Cu<sup>2+</sup> and Pb<sup>2+</sup> adsorption on the biochars fitted by the linear Langmuir and  
 42  
 43 Freundlich isotherm models.  
 44  
 45  
 46

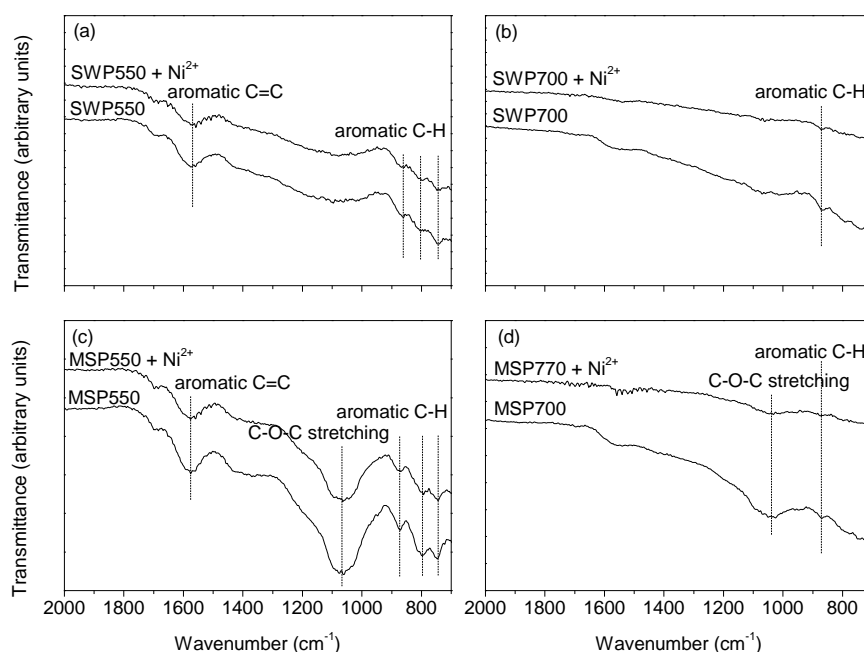
Metal	Biochar	Langmuir			Freundlich		
		Q <sub>max</sub> (mmol/g)	b (L/mmol)	R <sup>2</sup>	K <sub>f</sub>	1/n	R <sup>2</sup>
Ni <sup>2+</sup>	SWP550	0.057	0.535	0.979	0.018	0.540	0.959

	SWP700	0.043	1.821	0.963	0.024	0.353	0.954
	MSP550	0.157	161.579	0.865	0.146	0.157	0.899
	MSP700	0.196	123.481	0.682	0.179	0.145	0.699
	SWP550	0.019	13.321	0.999	0.017	0.088	0.955
	SWP700	0.086	4.785	0.985	0.061	0.226	0.980
Cu <sup>2+</sup>	MSP550	0.130	133.062	0.999	0.112	0.103	0.275
	MSP700	0.229	351.633	0.994	0.198	0.233	0.343
	SWP550	0.039	33.437	0.999	0.037	0.081	0.904
	SWP700	0.079	909.290	0.9999	0.074	0.079	0.375
Pb <sup>2+</sup>	MSP550	0.183	-407.054	0.9998	0.164	0.151	0.467
	MSP700	0.357	23.907	0.998	0.318	0.315	0.451

### 3.6 Adsorption mechanisms and discussion

Biochar can adsorb heavy metals through a range of mechanisms including physical sorption, cation exchange, cation- $\pi$  interaction, surface complexation and surface precipitation (Shen et al. 2017b). The FT-IR spectra (Fig. 5) generally show slight decrease of the peaks representing aromatic C=C and aromatic C-H of all four biochars after Ni<sup>2+</sup> adsorption. This suggests that

1 cation- $\pi$  interaction, which is closely related to aromatic C (Keiluweit and  
2  
3  
4 Kleber 2009), may be a mechanism for  $\text{Ni}^{2+}$  adsorption on the four biochars.  
5  
6  
7 The peaks representing C-O-C stretching also decreased after  $\text{Ni}^{2+}$  adsorption  
8  
9  
10 for MSP derived biochars. This C-O-C belongs to acid derivatives (Keiluweit  
11  
12 2010), suggesting cation exchange or complexation, associated with acidic  
13  
14  
15 groups, may also contribute to  $\text{Ni}^{2+}$  adsorption on MSP derived biochars.  
16  
17  
18  
19  
20



21  
22  
23  
24  
25  
26  
27  
28  
29  
30  
31  
32  
33  
34  
35  
36  
37  
38  
39  
40  
41  
42  
43  
44  
45 Fig. 5. FT-IR spectra of biochars before and after  $\text{Ni}^{2+}$  adsorption (the post  $\text{Ni}^{2+}$   
46  
47 adsorption sample was obtained from those for isotherm tests at 5 mM).  
48  
49  
50

51  
52 A previous study observed that surface precipitation and cation- $\pi$  interaction  
53  
54 are the main mechanisms contributing to heavy metal adsorption for biochars  
55  
56 produced from other feedstocks (wheat straw and rice husk) but under the  
57  
58  
59  
60  
61  
62  
63  
64  
65

1 same production processes as those used in the present study (Shen et al.  
2  
3 2017b). In the present study, the high solution-pH dependence of the  
4  
5 adsorption capacity of the four biochars for Ni<sup>2+</sup> (Fig. 4) suggests that surface  
6  
7 precipitation or cation- $\pi$  interaction are the primary adsorption mechanisms,  
8  
9 as they are both highly pH-dependent. As mentioned above, wood typically  
10  
11 has higher lignin content than does *miscanthus*, but lower inorganic minerals.  
12  
13 The incomplete carbonation of the feedstock during production of biochar, due  
14  
15 to more ligneous material which is more thermally resistant, can result SWP  
16  
17 derived biochars with less alkaline minerals (e.g., K<sub>2</sub>O) (Dodson 2011), as is  
18  
19 indicated by lower pH (Table 1) as well as in lower contents of inorganic  
20  
21 compounds (e.g. CO<sub>3</sub><sup>2-</sup> and PO<sub>4</sub><sup>3-</sup>) for metal precipitation.  
22  
23  
24  
25  
26  
27  
28  
29  
30

31  
32 Therefore, SWP derived biochars may have adsorbed Ni<sup>2+</sup> through surface  
33  
34 precipitation and cation- $\pi$  interaction. In comparison, MSP derived biochars  
35  
36 may have stronger ability to precipitate Ni<sup>2+</sup> compared with SWP. MSP derived  
37  
38 biochars may also adsorb Ni<sup>2+</sup> through cation exchange and surface  
39  
40 complexation, in addition to precipitation and cation- $\pi$  interaction. Therefore,  
41  
42 SWP derived biochars have lower adsorption capacities for Ni<sup>2+</sup> and other two  
43  
44 metals as compared with MSP. This indicates that feedstock type is an  
45  
46 important factor affecting the adsorption capacities of biochars for heavy  
47  
48 metals.  
49  
50  
51  
52  
53  
54  
55  
56  
57  
58

1 For the same feedstock, a higher production temperature generally results in a  
2  
3  
4 higher adsorption capacity for the metals (Table 2). Higher production  
5  
6 temperature promotes the carbonisation process of the feedstock and  
7  
8 therefore aids the formation of more alkaline minerals, which will aid in the  
9  
10 precipitation of metals to biochar surfaces. Although the pH and ash content  
11  
12 were not significantly different between MSP550 and MSP700, the significantly  
13  
14 lower O/C and H/C values for MSP700 suggests a higher degree of  
15  
16 carbonisation and a higher aromaticity, which could provide MSP700 more  
17  
18 aromatic  $\pi$  electrons for cation- $\pi$  interactions with the metals (Keiluweit and  
19  
20 Kleber 2009).  
21  
22  
23  
24  
25  
26  
27  
28

29  
30 Apart from the adsorption capacity, the kinetics of metal uptake and the  
31  
32 influence of solution pH on the degree of metal adsorption are similar for SWP  
33  
34 and MSP derived biochars. Biochars produced from wheat straw and rice husk  
35  
36 under the same standardised production process in a previous study (Shen et  
37  
38 al. 2017c) also show similar trends in terms of kinetics and the influence of  
39  
40 solution pH to  $\text{Ni}^{2+}$  adsorption. The faster kinetics of removal may be due to the  
41  
42 small particle size of the biochars and the relatively high initial sorbate  
43  
44 concentrations in solutions in both of the two studies.  
45  
46  
47  
48  
49  
50  
51

#### 52 53 54 4 Conclusions 55 56

57 This study investigates the adsorption characteristics of  $\text{Ni}^{2+}$ ,  $\text{Cu}^{2+}$  and  $\text{Pb}^{2+}$  on  
58

1 SWP and MSP derived biochars. The kinetics study shows that the adsorption  
2  
3 of Ni<sup>2+</sup> to all four biochars reached equilibrium rapidly (within 5 minutes),  
4  
5 regardless of feedstock type and production temperature, which may be due to  
6  
7 the small particle size of the biochars and relatively high initial sorbate  
8  
9 concentrations in solutions. Likewise, the solution-pH dependence of Ni<sup>2+</sup>  
10  
11 adsorption for the four biochars shows a similar trend. There was an initial  
12  
13 solution pH range of approximately 3-8, within which both the Ni<sup>2+</sup> removal  
14  
15 percentage and equilibrium solution pH remained nearly constant. This was  
16  
17 due to a nearly constant equilibrium solution pH within the range, which  
18  
19 resulted from the buffering effect of the biochars. Between the initial solution pH  
20  
21 range of 8-10, the Ni<sup>2+</sup> removal percentage dramatically increased to nearly  
22  
23 100%, corresponding to increased equilibrium solution pH. In general, the  
24  
25 adsorption of Ni<sup>2+</sup> on the four biochars was highly dependent on equilibrium  
26  
27 solution pH. The biggest difference between the adsorption characteristics of  
28  
29 SWP and MSP derived biochars are their adsorption capacities for all three  
30  
31 metals. MSP derived biochars have significantly higher Q<sub>max</sub> values than do  
32  
33 those produced from SWP. Lignin and inorganic mineral contents may be the  
34  
35 primary factors that cause the differences of adsorption capacity between  
36  
37 SWP and MSP derived biochars.  
38  
39  
40  
41  
42  
43  
44  
45  
46  
47  
48  
49  
50  
51  
52  
53

54  
55  
56 Our study indicates that feedstock type is a primary factor affecting the  
57  
58



1 adsorption capacities of biochar for heavy metals. As this study only includes  
2  
3 adsorption studies, the influence of feedstock type on the  
4  
5 desorption/reusability of the biochars are suggested for future work. More  
6  
7 testing methods (e.g., X-ray absorption and X-ray diffraction) and surface  
8  
9 complexation modelling may be used to aid in determining the mechanistic  
10  
11 driving forces impacting the adsorption capacities of biochar for heavy metals  
12  
13 in future studies.  
14  
15  
16  
17  
18  
19  
20

## 21 Acknowledgements

22  
23  
24  
25 The standard biochars were obtained from the UK Biochar Research Centre  
26  
27 (UKBRC) at the University of Edinburgh. The authors would like to thank Dr.  
28  
29 Ondrej Masek from the UKBRC for his kind help in preparing and delivering  
30  
31 the biochar samples. Special thanks also go to Dr. Zhen Li from the College of  
32  
33 Resources and Environmental Sciences, Nanjing Agricultural University, China,  
34  
35 who conducted the SEM imaging for the biochars used in this study. The  
36  
37 authors would also like to thank Tiesheng Wang and Rui Wu from the  
38  
39 Department of Materials Science and Metallurgy at the University of  
40  
41 Cambridge for conducting the FT-IR tests. The first author would like to thank  
42  
43 the Killam Trusts from Canada for kindly providing the Izaak Walton Killam  
44  
45 Memorial Postdoctoral Fellowship.  
46  
47  
48  
49  
50  
51  
52  
53  
54  
55  
56  
57  
58

1          References  
2  
3

4          Beesley L, Moreno-Jiménez E, Gomez-Eyles JL, et al (2011) A review of  
5  
6                  biochars' potential role in the remediation, revegetation and restoration of  
7  
8                  contaminated soils. Environ Pollut 159:3269–82. doi:  
9  
10                 10.1016/j.envpol.2011.07.023  
11  
12

13  
14  
15          Cao X, Ma L, Liang Y, et al (2011) Simultaneous immobilization of lead and  
16                  atrazine in contaminated soils using dairy-manure biochar. Environ Sci  
17                  Technol 45:4884–9. doi: 10.1021/es103752u  
18  
19  
20  
21

22  
23  
24          Chi T, Zuo J, Liu F (2017) Performance and mechanism for cadmium and lead  
25                  adsorption from water and soil by corn straw biochar. Front Environ Sci  
26                  Eng. doi: 10.1007/s11783-017-0921-y  
27  
28  
29  
30

31  
32          Chotpantarat S, Ong SK, Sutthirat C, Osathaphan K (2011) Competitive  
33                  sorption and transport of  $Pb^{2+}$ ,  $Ni^{2+}$ ,  $Mn^{2+}$ , and  $Zn^{2+}$  in lateritic soil  
34                  columns. J Hazard Mater 190:391–396. doi:  
35                  10.1016/j.jhazmat.2011.03.058  
36  
37  
38

39  
40          Choy KKH, Ko DCK, Cheung CW, et al (2004) Film and intraparticle mass  
41                  transfer during the adsorption of metal ions onto bone char. J Colloid  
42                  Interface Sci 271:284–295. doi: 10.1016/j.jcis.2003.12.015  
43  
44  
45  
46

47          Cui L, Yan J, Li L, et al (2015) Does Biochar Alter the Speciation of Cd and Pb  
48  
49  
50  
51  
52

1 in Aqueous Solution? BioResources. 10:88–104.

2  
3  
4 Dodson J (2011) Wheat straw ash and its use as a silica source. Ph.D. thesis  
5  
6  
7 dissertation. University of York.

8  
9  
10 Foo KY, Hameed BH (2010) Insights into the modeling of adsorption isotherm  
11  
12  
13 systems. Chem Eng J 156:2–10. doi: 10.1016/j.cej.2009.09.013  
14  
15

16  
17 Gillman G, Sumpter E (1986) Modification to the compulsive exchange method  
18  
19  
20 for measuring exchange characteristics of soils. Aust J Soil Res 24:61. doi:  
21  
22  
23 10.1071/SR9860061  
24

25  
26 Hou D, Al-Tabbaa A (2014) Sustainability: A new imperative in contaminated  
27  
28  
29 land remediation. Environ Sci Policy 39:25–34. doi:  
30  
31  
32 10.1016/j.envsci.2014.02.003  
33  
34

35  
36 Hou D, Ding Z, Li G, et al A Sustainability Assessment Framework for  
37  
38  
39 Agricultural Land Remediation in China.  
40

41  
42 Hou D, Gu Q, Ma F, O'Connell S (2016) Life cycle assessment comparison of  
43  
44  
45 thermal desorption and stabilization/solidification of mercury contaminated  
46  
47  
48 soil on agricultural land. J Clean Prod 139:949–956. doi:  
49  
50  
51 10.1016/j.jclepro.2016.08.108  
52  
53

54 Hou D, Li F Complexities Surrounding China's Soil Action Plan. L Degrad Dev.  
55  
56  
57  
58

1 Hou D, O'Connor D, Nathanail P, et al (2017a) Integrated GIS and multivariate  
2  
3 statistical analysis for regional scale assessment of heavy metal soil  
4  
5 contamination: A critical review.  
6  
7

8  
9  
10 Hou D, Qi S, Zhao B, et al (2017b) Incorporating life cycle assessment with  
11  
12 health risk assessment to select the “greenest” cleanup level for Pb  
13  
14 contaminated soil. J Clean Prod 162:1157–1168. doi:  
15  
16 10.1016/j.jclepro.2017.06.135  
17  
18  
19

20  
21  
22 Inyang MI, Gao B, Yao Y, et al (2015) A Review of Biochar as a Low-Cost  
23  
24 Adsorbent for Aqueous Heavy Metal Removal. Crit Rev Environ Sci  
25  
26 Technol 00–00. doi: 10.1080/10643389.2015.1096880  
27  
28  
29

30  
31 Jahirul MI, Rasul MG, Chowdhury AA, Ashwath N (2012) Biofuels production  
32  
33 through biomass pyrolysis- A technological review. Energies 5:4952–5001.  
34  
35 doi: 10.3390/en5124952  
36  
37  
38

39  
40  
41 Keiluweit M, Kleber M (2009) Molecular-level interactions in soils and  
42  
43 sediments: The role of aromatic  $\pi$ -systems. Environ Sci Technol  
44  
45 43:3421–3429. doi: 10.1021/es8033044  
46  
47  
48

49  
50 Keiluweit M, Nico PS, Johnson M, Kleber M (2010) Dynamic molecular  
51  
52 structure of plant biomass-derived black carbon (biochar). Environ Sci  
53  
54 Technol 44:1247–1253. doi: 10.1021/es9031419  
55  
56  
57

1 Lehmann J (2007) Bio-energy in the black. Front Ecol Environ preprint:1. doi:

2  
3 10.1890/060133  
4  
5

6  
7 Li H, Dong X, da Silva EB, et al (2017) Mechanisms of metal sorption by  
8

9 biochars: Biochar characteristics and modifications. Chemosphere  
10

11 178:466–478. doi: 10.1016/j.chemosphere.2017.03.072  
12  
13

14  
15  
16 Liu P, Liu WJ, Jiang H, et al (2012a) Modification of bio-char derived from fast  
17

18 pyrolysis of biomass and its application in removal of tetracycline from  
19

20 aqueous solution. Bioresour Technol 121:235–240. doi:  
21

22 10.1016/j.biortech.2012.06.085  
23  
24

25  
26  
27  
28 Liu W, Wang T, Borthwick AGL, et al (2013) Adsorption of Pb<sup>2+</sup>, Cd<sup>2+</sup>, Cu<sup>2+</sup>  
29

30 and Cr<sup>3+</sup> onto titanate nanotubes: Competition and effect of inorganic  
31

32 ions. Sci Total Environ 456–457:171–180. doi:  
33

34 10.1016/j.scitotenv.2013.03.082  
35  
36  
37

38  
39  
40 Liu Y, Zhao X, Li J, et al (2012b) Characterization of bio-char from pyrolysis of  
41

42 wheat straw and its evaluation on methylene blue adsorption. Desalin  
43

44 Water Treat 46:115–123. doi: 10.1080/19443994.2012.677408  
45  
46  
47

48  
49  
50 Ma F, Peng C, Hou D, et al (2015) Citric acid facilitated thermal treatment: An  
51

52 innovative method for the remediation of mercury contaminated soil. J  
53

54 Hazard Mater 300:546–552. doi: 10.1016/j.jhazmat.2015.07.055  
55  
56  
57

- 1 Ma F, Zhang Q, Xu D, et al (2014) Mercury removal from contaminated soil by  
2  
3 thermal treatment with FeCl<sub>3</sub> at reduced temperature. Chemosphere  
4  
5  
6 117:388–393. doi: 10.1016/j.chemosphere.2014.08.012  
7  
8  
9
- 10 Mohan D, Kumar H, Sarswat A, et al (2014) Cadmium and lead remediation  
11  
12 using magnetic oak wood and oak bark fast pyrolysis bio-chars. Chem  
13  
14 Eng J 236:513–528. doi: 10.1016/j.cej.2013.09.057  
15  
16  
17  
18
- 19 Mohan D, Pittman CU, Bricka M, et al (2007) Sorption of arsenic, cadmium,  
20  
21 and lead by chars produced from fast pyrolysis of wood and bark during  
22  
23 bio-oil production. J Colloid Interface Sci 310:57–73. doi:  
24  
25 10.1016/j.jcis.2007.01.020  
26  
27  
28  
29  
30
- 31 Park J-H, Cho J-S, Ok YS, et al (2015) Comparison of single and competitive  
32  
33 metal adsorption by pepper stem biochar. Arch Agron Soil Sci  
34  
35 340:150717092443002. doi: 10.1080/03650340.2015.1074186  
36  
37  
38  
39  
40
- 41 Qi S, Hou D, Luo J (2017) Optimization of groundwater sampling approach  
42  
43 under various hydrogeological conditions using a numerical simulation  
44  
45 model. J Hydrol 552:505–515.  
46  
47  
48  
49
- 50 Rees F, Simonnot MO, Morel JL (2014) Short-term effects of biochar on soil  
51  
52 heavy metal mobility are controlled by intra-particle diffusion and soil pH  
53  
54 increase. Eur J Soil Sci 65:149–161. doi: 10.1111/ejss.12107  
55  
56  
57  
58

- 1 Ronsse F, van Hecke S, Dickinson D, Prins W (2013) Production and  
2  
3 characterization of slow pyrolysis biochar: influence of feedstock type and  
4  
5 pyrolysis conditions. *GCB Bioenergy* 5:104–115. doi: 10.1111/gcbb.12018  
6  
7  
8  
9
- 10 Saleh ME, El-Refaey AA, Mahmoud AH (2016) Effectiveness of sunflower  
11  
12 seed husk biochar for removing copper ions from wastewater: a  
13  
14 comparative study. *Soil Water Res* 11:53–63. doi:  
15  
16 10.17221/274/2014-SWR  
17  
18  
19  
20  
21
- 22 Shen Z, Jin F, Wang F, et al (2015) Sorption of lead by Salisbury biochar  
23  
24 produced from British broadleaf hardwood. *Bioresour Technol* 193:553–  
25  
26 556. doi: 10.1016/j.biortech.2015.06.111  
27  
28  
29  
30
- 31 Shen Z, Som AM, Wang F, et al (2016) Long-term impact of biochar on the  
32  
33 immobilisation of nickel (II) and zinc (II) and the revegetation of a  
34  
35 contaminated site. *Sci Total Environ* 542:771–776.  
36  
37  
38  
39  
40
- 41 Shen Z, Tian D, Zhang X, et al (2017a) Mechanisms of biochar assisted  
42  
43 immobilization of Pb 2+ by bioapatite in aqueous solution. *Chemosphere*  
44  
45 190: 260-266. doi: 10.1016/j.chemosphere.2017.09.140  
46  
47  
48  
49
- 50 Shen Z, Zhang Y, Jin F, et al (2017b) Qualitative and quantitative  
51  
52 characterisation of adsorption mechanisms of lead on four biochars. *Sci*  
53  
54 *Total Environ* 609:1401–1410. doi: 10.1016/j.scitotenv.2017.08.008  
55  
56  
57  
58

- 1 Shen Z, Zhang Y, McMillan O, et al (2017c) Characteristics and mechanisms  
2  
3 of nickel adsorption on biochars produced from wheat straw pellets and  
4  
5 rice husk. *Environ Sci Pollut Res* 1–11. doi: 10.1007/s11356-017-8847-2  
6  
7  
8  
9
- 10 Song Y, Hou D, Zhang J, et al (2018) Environmental and socio-economic  
11  
12 sustainability appraisal of contaminated land remediation strategies: A  
13  
14 case study at a mega-site in China. *Sci Total Environ* 610–611:391–401.  
15  
16  
17 doi: 10.1016/j.scitotenv.2017.08.016  
18  
19  
20  
21
- 22 Tran HN, You S-J, Chao H-P (2016) Effect of pyrolysis temperatures and times  
23  
24 on the adsorption of cadmium onto orange peel derived biochar. *Waste  
25  
26 Manag Res* 34:129–138. doi: 10.1177/0734242X15615698  
27  
28  
29  
30
- 31 Uchimiya M, Cantrell KB, Hunt PG, et al (2012) Retention of Heavy Metals in a  
32  
33 Typic Kandudult Amended with Different Manure-based Biochars. *J  
34  
35 Environ Qual* 41:1138. doi: 10.2134/jeq2011.0115  
36  
37  
38  
39  
40
- 41 Usman A, Sallam A, Zhang M, et al (2016) Sorption Process of Date Palm  
42  
43 Biochar for Aqueous Cd (II) Removal: Efficiency and Mechanisms. *Water  
44  
45 Air Soil Pollut*. doi: 10.1007/s11270-016-3161-z  
46  
47  
48  
49
- 50 Wang Z, Han L, Sun K, et al (2016) Sorption of four hydrophobic organic  
51  
52 contaminants by biochars derived from maize straw, wood dust and swine  
53  
54 manure at different pyrolytic temperatures. *Chemosphere* 144:285–291.  
55  
56  
57  
58



1 doi: 10.1016/j.chemosphere.2015.08.042  
2  
3

4 Zhang H, Chen C, Gray EM, Boyd SE (2017a) Effect of feedstock and  
5  
6  
7 pyrolysis temperature on properties of biochar governing end use efficacy.  
8  
9  
10 Biomass and Bioenergy 105:136–146. doi:  
11  
12 10.1016/j.biombioe.2017.06.024  
13  
14  
15

16 Zhang P, Lo I, O'Connor D, et al (2017b) High efficiency removal of methylene  
17  
18  
19 blue using SDS surface-modified ZnFe<sub>2</sub>O<sub>4</sub> nanoparticles. J Colloid  
20  
21  
22 Interface Sci 508:39–48.  
23  
24  
25  
26  
27  
28  
29  
30  
31  
32  
33  
34  
35  
36  
37  
38  
39  
40  
41  
42  
43  
44  
45  
46  
47  
48  
49  
50  
51  
52  
53  
54  
55  
56  
57  
58  
59  
60  
61  
62  
63  
64  
65